Astron. Astrophys. 339, 575–586 (1998)

ASTRONOMY
AND
ASTROPHYSICS

The biconical cavity associated with HD 200775: the formation of a cometary nebula

A. Fuente[1], **J. Martín-Pintado**[1], **A. Rodríguez-Franco**[2], **and G.D. Moriarty-Schieven**[3]

[1] Observatorio Astronómico Nacional (IGN), Campus Universitario, Apdo. 1143, E-28800 Alcalá de Henares (Madrid),Spain
[2] Universidad Complutense de Madrid, Av. Arcos de Jalón s/n, E-28037 Madrid, Spain
[3] Joint Astronomy Centre, 660 N. A'ohoku Place, Hilo, HI 96720, USA

Received 15 June 1998 / Accepted 3 September 1998

Abstract. We have observed with high angular resolution (10″ – 24″) an area of $\approx 18' \times 15'$ around HD 200775 in the J=2→1 line of ^{12}CO and the J=1→0 lines of ^{13}CO and C^{18}O. An interferometric HI 21cm image with similar angular resolution (14″) is also presented. Molecular observations show that the star is located in a biconical cavity that has been very likely excavated by an energetic and bipolar outflow in an earlier evolutionary stage. The star is not located at the apex of this cavity but $\sim$ 50 ″ towards the eastern lobe. At the present stage, there is no evidence for high velocity gas within the lobes of the cavity. However, the morphology of the HI emission, two filaments arranged in a "$>$" shape feature, and the bow shock located at the tip of one of these filaments, show that high velocity atomic gas is outflowing in a shell adjacent to the walls of the cavity in the eastern lobe. Since this high velocity atomic gas has not been detected in the western lobe, the outflow has a cometary shape. We propose that this outflow is formed when the atomic gas in the inner walls of the cavity is accelerated by the stellar wind. The cometary shape is due to the off-center position of the star. This cometary HI region constitutes the latest evolutionary stage of the bipolar outflow associated with HD 200775. Based on these results we propose a simple model to explain the formation of cometary nebulae in massive star forming regions.

Key words: stars: individual: HD 200775 – stars: pre-main-sequence – ISM: jets and outflows – ISM: individual objects: NGC 7023 – reflection nebulae – radio lines: ISM

1. Introduction

Mass-loss phenomena are associated with the early stages of star formation both in low-mass and high-mass objects. In the last decade, a big observational and theoretical effort has been made to understand the structure and evolution of the outflows associated with low-mass YSOs. But very few works have been done to understand the intermediate and high-mass outflows. This is due mainly to observational problems: i) Massive star forming regions are located further away than low-mass star forming regions; ii) High-mass stars are usually formed in clusters where several stars could be driving bipolar outflows at the same time; iii) The creation and expansion of ionized regions increase the confusion when studying the kinematics of these massive regions; and finally iv) because of the fast evolution of high-mass stars, the mass-loss phase is expected to be shorter than in low-mass stars.

Herbig Ae-Be (HAEBE) stars are intermediate mass (1 – 10 $M_\odot$) pre-main sequence stars. They are associated with reflection nebulosities and obscuration regions, and share characteristics with T Tau and OB stars. Like low-mass stars, these objects present large IR, mm and submm continuum excess, rapid photometric and spectroscopy variability, stellar winds, and high velocity molecular outflows (see Catala, 1989 for a review). Like the more massive OB stars, some of these stars are formed in clusters. These stars are unable to create extended HII regions, but large HI regions can be found associated with some of them (Fuente et al. 1993, 1996, 1998; Blouin et al. 1997). Therefore, only a combined study of the atomic and molecular gas can provide a picture of the region. Although the star forming regions are located closer to the sun and are less complex than those of OB stars, very few intermediate-mass outflows have been studied in detail. Furthermore, none of these outflows has been studied combining the atomic and molecular data. The study of these outflows can give important clues for the understanding of the more massive outflows.

HD 200775 is a B3 star located at the northern edge of an elongated molecular cloud. Located at a distance of 430 pc (van den Ancker et al. 1997), it is the illuminating star of the well-known reflection nebula NGC 7023. The existence of a bipolar outflow associated with this star was first proposed by Watt et al. (1986) based on their low-angular resolution ^{12}CO maps. Large scale maps of the region in ^{13}CO show that the star is located in a biconical cavity whose walls delineate perfectly the borders of the optical nebula (Fuente et al. 1992). The shape of this cavity strongly suggests that a bipolar outflow has excavated it. Rogers et al. (1995) carried out an interferometric image of this nebula in the HI 21cm line with an angular resolution of $\sim$1'. They found that the HI emission is filling the molecular cavity and that the density inside the cavity is at least one order of magnitude lower than the density in the surrounding molecular

Send offprint requests to: A. Fuente

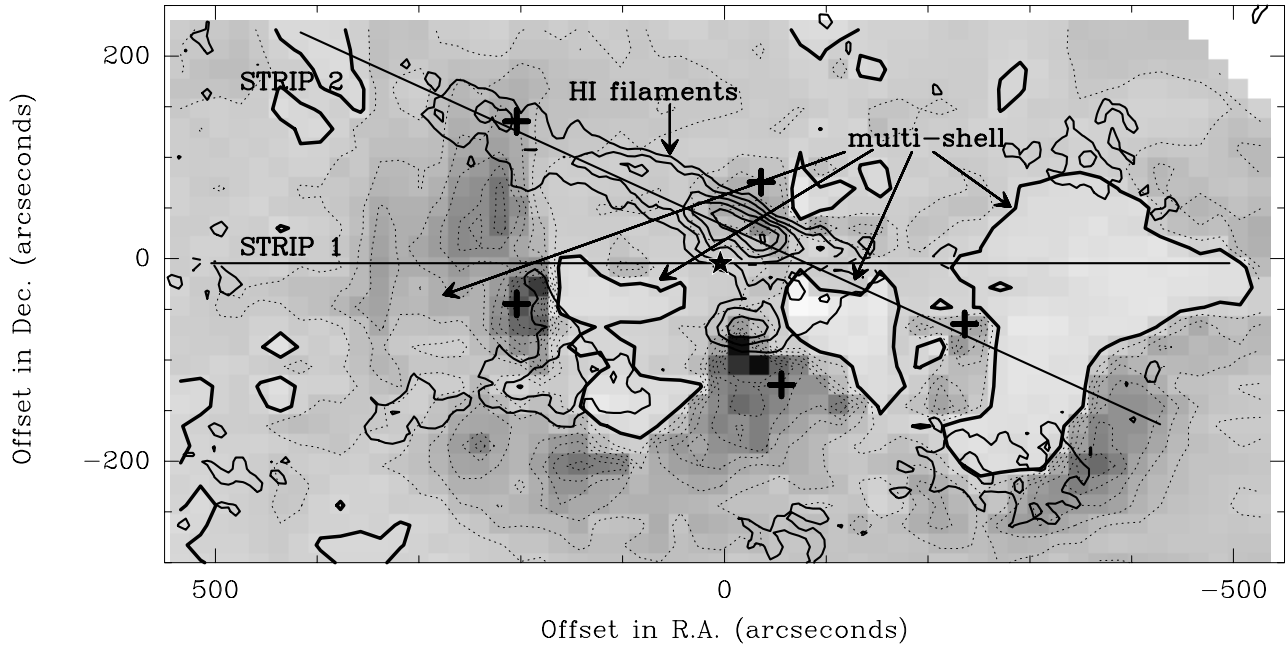

Fig. 1. Scheme with the main features observed in the HI and ^{12}CO emissions towards NGC 7023. The grey scale and dashed contours corresponds to the integrated intensity of the ^{12}CO J=2→1 line at a velocity of 1.86 kms^{-1}. The thick contours indicates the HI filaments and the multi-shell structure observed in ^{12}CO. The star position is marked with a star. Crosses mark the selected positions for which we have estimated the physical conditions (see Table 1). The lines indicate the strips shown in Fig. 9. The (0,0) position is RA: $21^h01^m00^s.0$ Dec: $67°58'00''.0$.

cloud. Since the gas around the star is mainly atomic, the atomic data are crucial to understanding the kinematics of the region. We have mapped a region of ≈ 18'×15' around the star with high angular resolution (beam ∼ 12″) in the J=2→1 rotational line of ^{12}CO and the HI 21cm line. These observations have allowed a study of the structure of the high velocity atomic and molecular gas of this nebula. Furthermore, in order to study the densest regions, we have mapped the same region in the J=1→0 rotational lines of ^{13}CO and C^{18}O.

2. Observations

We have observed an area of ≈ 18′×15′ around HD 200775 with a spacing of 20″ in the J=2→1 line of ^{12}CO and the J=1→0 line of ^{13}CO and C^{18}O. Observations were carried out in 1989 June, 1996 September and 1997 September using the 30-m IRAM telescope. The three lines have been observed simultaneously in order to avoid pointing and relative calibration problems. The half-power beam width of the telescope is 24″ and 10″ at 3mm and 1.3mm respectively. The forward and main beam efficiencies are respectively 0.92 and 0.68 at 3mm and 0.86 and 0.39 at 1.3mm. The observation procedure was position switching with the off-position 30′ east from the source. The spectrometers used in the observations were a 256×100 kHz filter bank and an autocorrelator split in two parts of 80 MHz of bandwidth and 78 kHz of spectral resolution. Typical system temperatures (in T_A^*) during the observations were 500-600 K at the frequency of the J=2→1 line of ^{12}CO, and around 200 K at the frequencies of the J=1→0 lines of ^{13}CO and C^{18}O. The line intensity scale is in units of T_A^* for all the data except in Fig. 6 and Sect. 3.2 in which we study the bow shock. Observations of atomic hydrogen were carried out on August 4 1993 using the Very Large Array (VLA) of the National Radio Astronomy Observatory[1] in its C configuration, providing a synthesized beam is 14″ and the spectral resolution of 0.644 kms^{-1} over 256 channels. These observations were described in detail and partially presented by Fuente et al. (1996). The data are presented in HI column density units calculated assuming optically thin emission.

3. Morphology and physical conditions

For clearness, we show in Figs. 1 and 2a summary with the main features observed in the molecular lines and HI maps. In Figs. 3, 4 and 5 we show the complete spectral maps of ^{12}CO, ^{13}CO and HI emissions respectively. In all the figures, the offsets are given relative to the position R.A.(1950)=21:01:00 Dec(1950)=67:58:00.0, offset (1.7″, 4.7″) from the star position. The spectra toward some selected positions are shown in Figs. 6, 7 and 8.

3.1. The cavity

Both molecular and atomic emission show that the star is located in a large (∼ 1.5 pc × 0.8 pc) cavity of the molecular cloud which is spatially coincident with the optical nebula. The shape of this cavity is biconical with the western lobe much larger than the eastern one, and the star located ∼ 50 ″ east from the apex of

[1] The National Radio Astronomy Observatory is operated by the Associated Universities, Inc. under contract with the National Science Foundation.

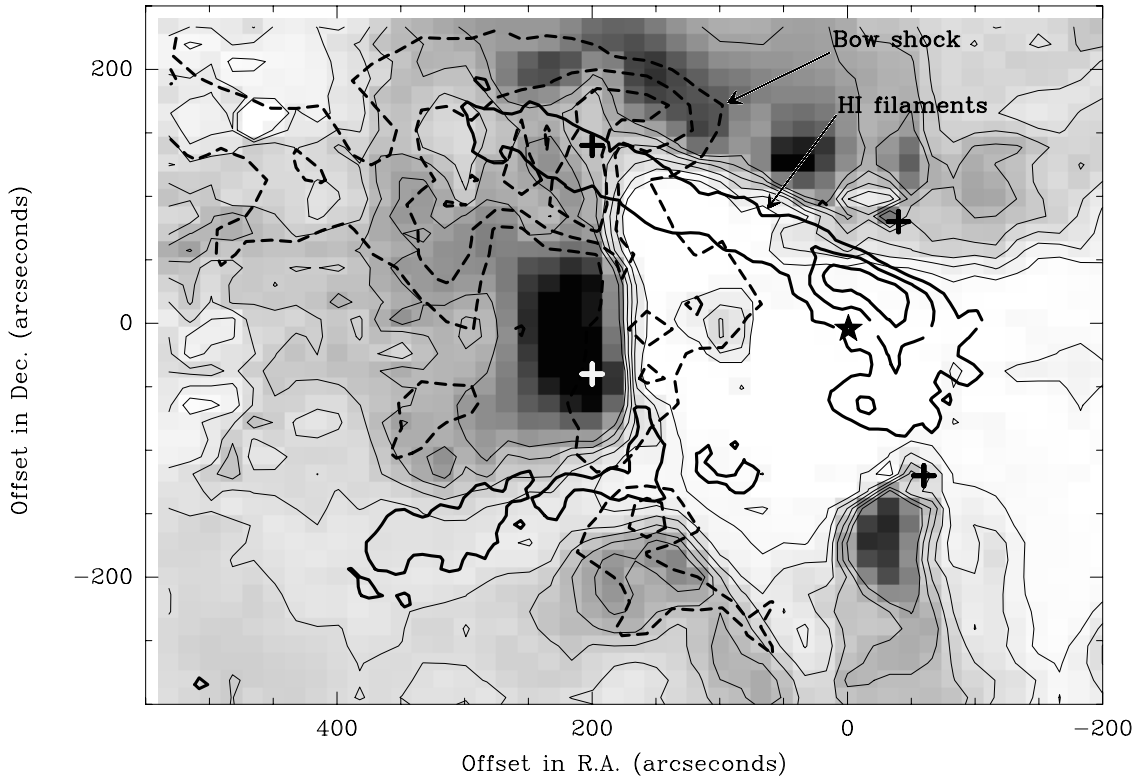

Fig. 2. Scheme with the main features observed in the HI and ^{12}CO and ^{13}CO emissions. The grey scale corresponds to the integrated intensity of the ^{13}CO J=1→0 line at a velocity of 1.86 kms^{-1}. The cavity and the tunnels are clearly seen in this map. The thick contours indicates the HI filaments which are spatially coincident with the ^{13}CO tunnels. The thick dashed contours corresponds to the integrated intensity of the ^{12}CO J=2→1 line at 3.79 kms^{-1} and clearly show the bow shock found at the tip of the northern HI filaments. The star and crosses mean the same as in Fig. 1.

the cavity (see Figs. 1 and 3). Within the cavity, the emission is not uniform. It presents a symmetric multi-shell structure that is better observed in the ^{12}CO emission (see Figs. 1 and 3). Close to the velocity of the ambient molecular cloud the ^{12}CO map shows the existence of a molecular filament that divides the western lobe in two subcavities. The first one has similar size to the eastern lobe and is located symmetric to it relative to the apex of the biconical cavity. The second subcavity seems also to have a counterpart beyond the intense eastern wall. But because of the complexity of this region, this tentative subcavity is not so clearly observed. The cavity is bordered by a bright rim in the ^{13}CO J=1→0 emission. Intense ^{13}CO clumps are found in this rim with the most intense located in the waist of the cavity and beyond the eastern wall. In this wall, the cavity shows two tunnels that penetrates into the molecular cloud (see Figs. 2 and 4). The straightness and direction of these tunnels suggest that they have been excavated by the outflow.

We have derived the gas column densities towards some selected positions in the walls of the cavity assuming a kinetic temperature of T_K = 30 K and a hydrogen density of n(H_2) = 5 10^3 cm^{-3} (as derived by Fuente et al. (1990,1993) from NH_3 and CO data) and fitting the observed lines with an LVG code. These positions are marked in Figs. 1 and 2 and the results are shown in Table 1. The derived ^{13}CO column densities are $\sim$ 1 – 3 10^{16} cm^{-2}. Within the cavity, the ^{13}CO column densities have been estimated assuming optically thin emission and a rotation temperature of 15 K (Rogers et al. 1995, Gerin et al. 1998). The obtained ^{13}CO column densities are also shown in Table 1 and the selected positions are marked in Figs. 1 and 2. The ^{13}CO column densities are $< 6\ 10^{15}$ cm^{-2} over the whole cavity, with a mean value of 1.6 10^{15} cm^{-2}. Then, the contrast between the walls and the interior of the cavity is of a factor > 10.

Both, in ^{12}CO and ^{13}CO emissions, the region present a bipolar structure. But the bipolarity turns into monopolarity in the HI image. The HI emission is formed by two intense filaments arranged in a ”>” shape feature with its apex spatially coincident with the apex of the molecular cavity (see Figs. 1, 2 and 5). These filaments have a length of $\approx$ 1 pc and run in straight lines adjacent to the walls of the eastern lobe of the cavity until they penetrate into the molecular cloud. Beyond the eastern wall, the HI filaments are spatially coincident with the tunnels detected in ^{13}CO emission. Assuming that the size of the filaments along the line of sight is the same as its thickness, the mean and peak hydrogen densities in the filaments are respectively $\sim 10^3$ cm^{-3} and $\sim 4\ 10^3$ cm^{-3}. These densities are two orders of magnitude larger than the mean hydrogen density estimated by Rogers et al. (1995) from a lower resolution HI image (synthesized beam $\approx 63.5'' \times 58.4''$). Therefore, the atomic gas is not filling the eastern lobe of the cavity with a uniform density. On the contrary, it is concentrated in a hollow

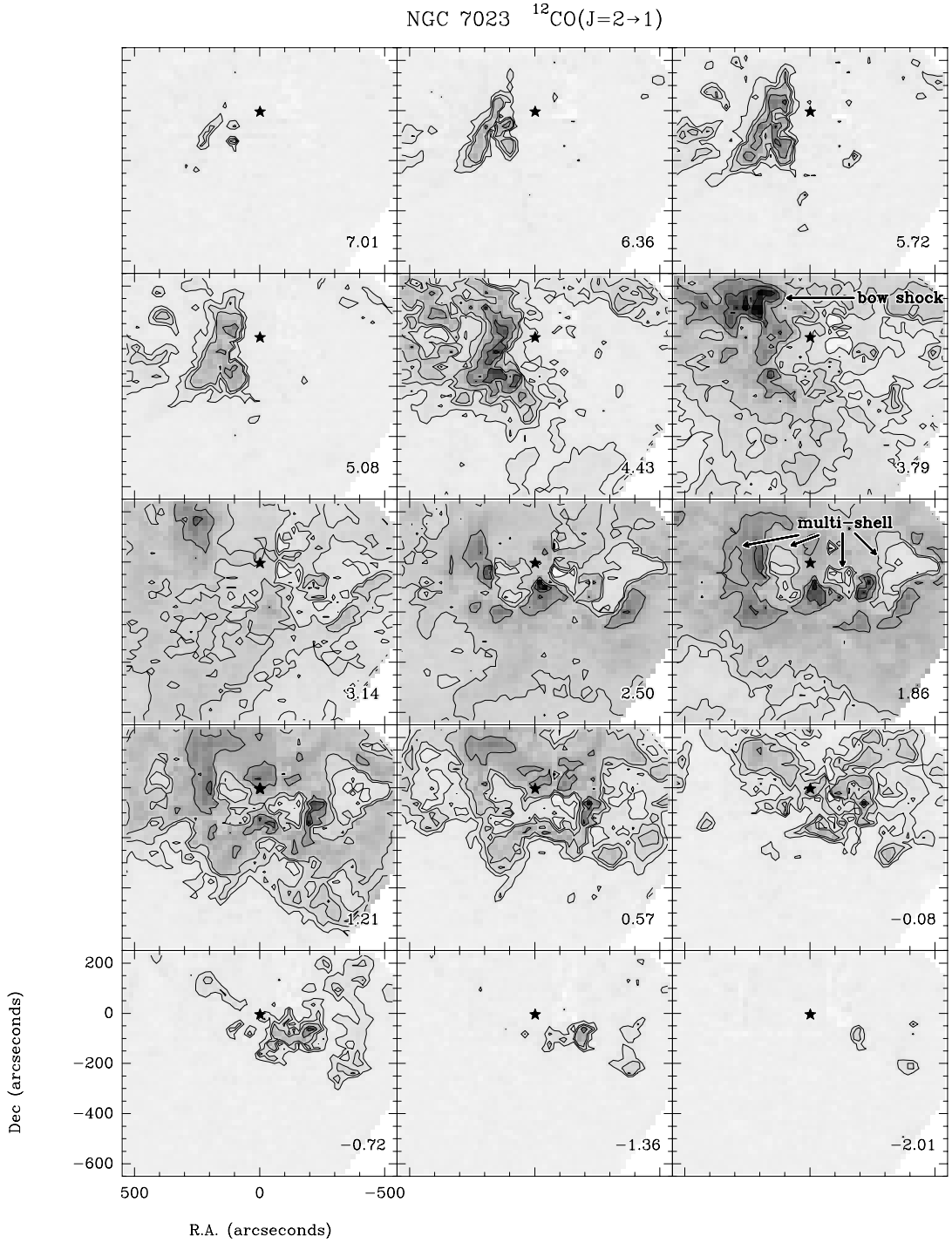

Fig. 3. Map of the integrated intensity map of the ^{12}CO J=2→1 line for different velocity intervals. The velocity interval is 0.644 kms^{-1}. Contour levels are 1, 2, 3 to 14 by 3 K kms^{-1}.

cone adjacent to the molecular walls. The HI filaments are the walls of this cone.

3.2. The bow shock

Our ^{12}CO maps show the existence of a very hot spot (T_{MB} (^{12}CO 2→1) ≈ 60 K) that is located at the tip of the northern HI filament (see the panel at 3.7 kms^{-1} in Fig. 3). The shape, high brightness temperature and location of this feature reminds a bow-shock. Since this hot spot is a relatively small region (thickness < 27″), we will use the main beam temperature to determine the physical conditions of the gas. In Fig. 8 we present the HI, ^{12}CO and ^{13}CO spectra towards this position [offset (200″, 140″)]. A narrow (Δv = 0.6 kms^{-1}) and intense

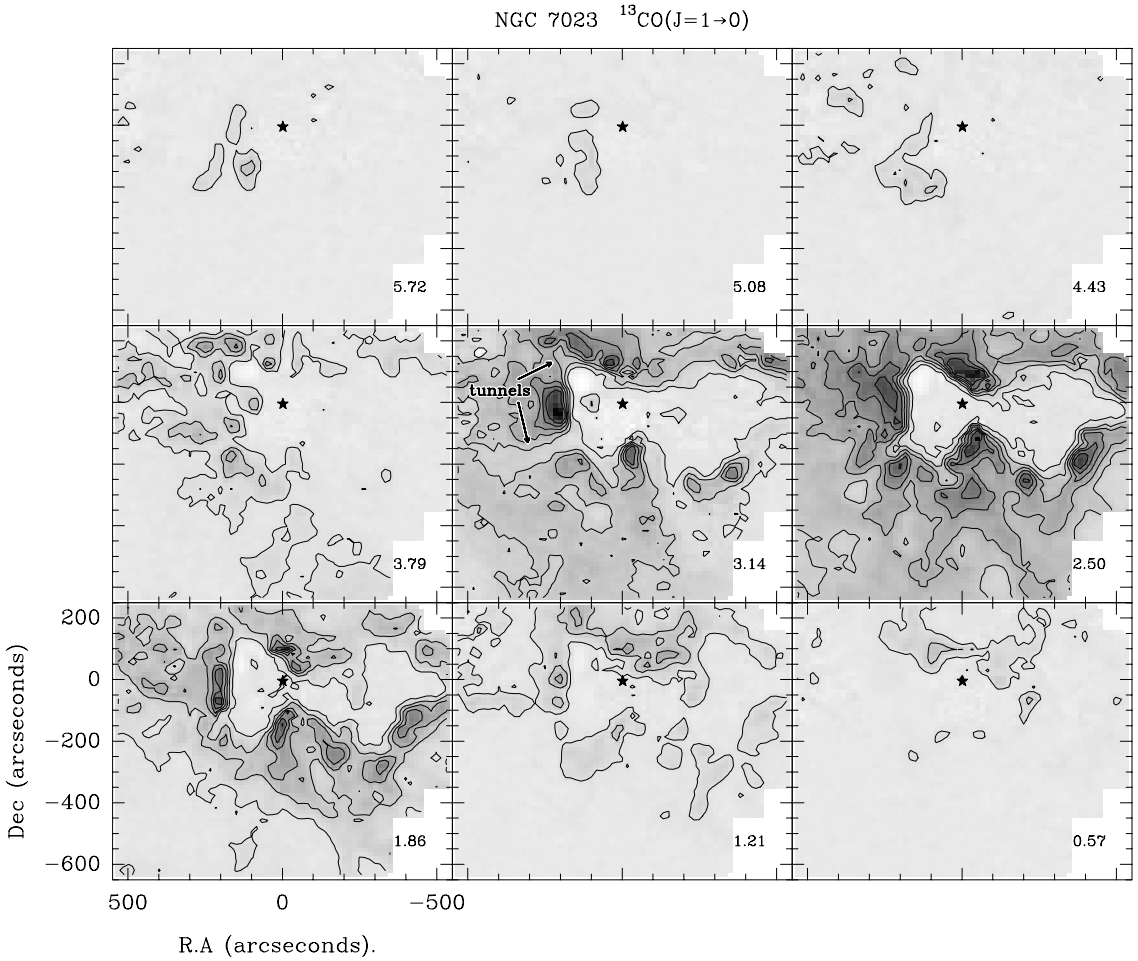

Fig. 4. The same as Fig. 3 for the ^{13}CO J=1→0 line. Contour levels are 0.5, 1.5 to 6 by 1 K kms^{-1}.

Table 1. Physical conditions

	Offset	T_K (K)	n(H_2) (cm^{-3})	N(^{13}CO) (cm^{-2})	N($C^{18}O$) (cm^{-2})
Cavity[1]	(0″, 0″)			2.1 10^{15}	
	(-240″, -60″)[2]			5.8 10^{15}	
	Mean			1.6 10^{15}	
Walls[3]	(-40″, 80″)	30	5.0 10^3	2.0 10^{16}	2.5 10^{15}
	(-60″, -120″)			1.3 10^{16}	1.5 10^{15}
	(200″, -40″)			3.3 10^{16}	1.7 10^{15}
Bow shock	(-200″, -140″)	>80		1.0 10^{15}	

[1] Within the cavity, the ^{13}CO column densities have been estimated assuming optically thin emission and a rotation temperature of 15 K.
[2] Position in the molecular filament that divides the western lobe in two subcavities.
[3] Physical conditions derived by fitting the ^{13}CO and $C^{18}O$ lines with an LVG code and assuming the physical conditions shown in the table.

line ($T_{MB}\approx$ 60 K) appears in the ^{12}CO J=2→1 spectrum at a velocity of $\sim$ 4 kms^{-1}, i.e., the velocity of the HI emission. The comparison between the ^{12}CO and ^{13}CO spectra shows that although the ^{12}CO is self-absorbed at the velocity of the ambient molecular cloud (2.5 kms^{-1}), the spike at $\sim$ 4 kms^{-1} is not due to self-absorption. In fact, this feature appears as a weak peak in the ^{13}CO J=1→0 spectrum. It is a well differentiated velocity component with a characteristic velocity (v $\sim$ 4 kms^{-1}) and a well defined spatial distribution (see the panel at 3.7 kms^{-1} in Fig. 3). Assuming a rotation temperature of 60 K and fitting this component in the ^{13}CO spectra, we derive a ^{13}CO column density of 10^{15} cm^{-2}. Therefore, this component corresponds to a extremely warm ($T_k > 80$ K) and thin ($A_v\sim$ 1 mag) layer of molecular gas, located at the tip of one of the HI filaments at a distance of 0.6 pc from the star. Following the bright rim that delineates the edge of the cavity, the bow-shock is located at the

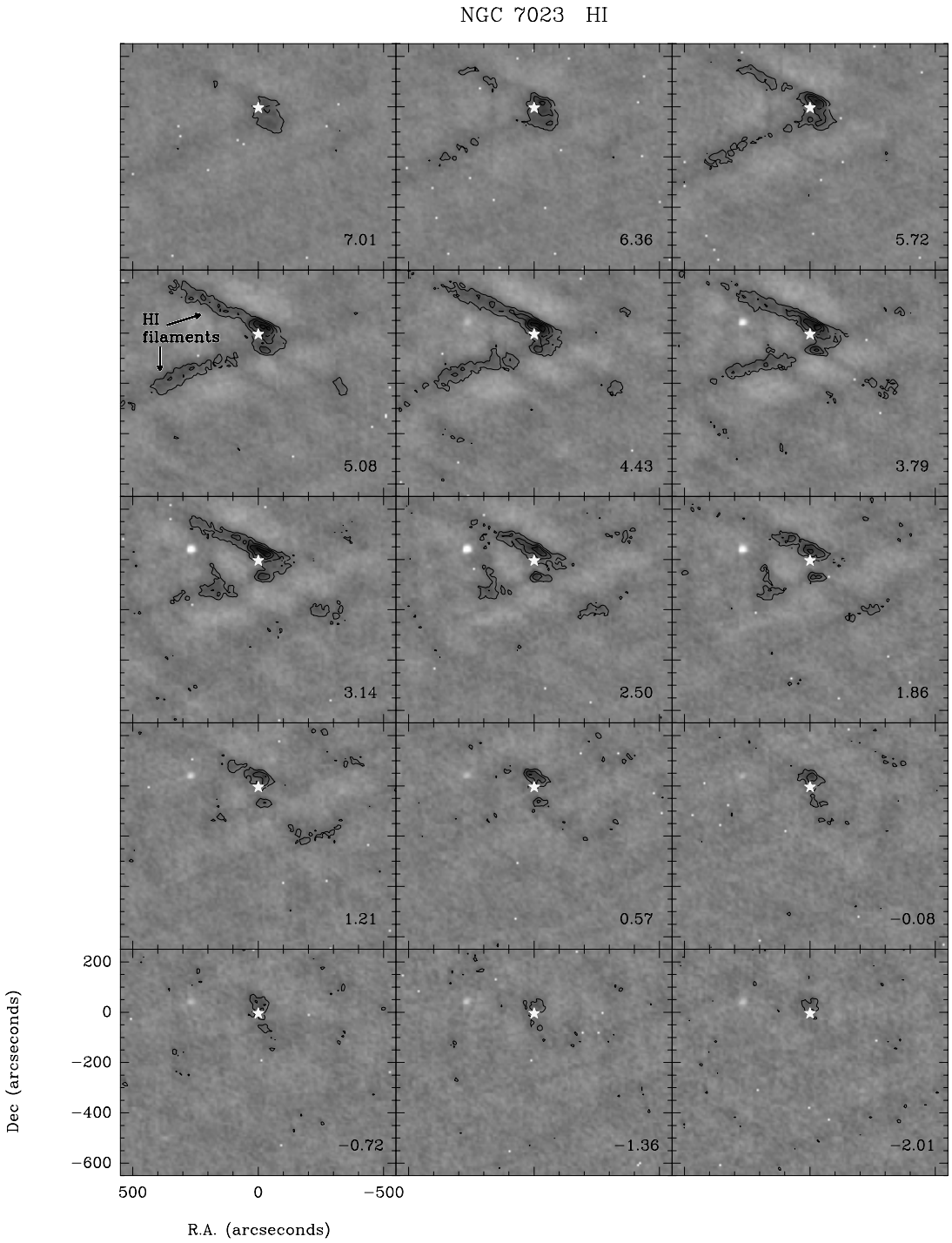

Fig. 5. Map of the HI column density for different velocity intervals towards NGC 7023. Contour levels are from 5.6 10^{20} to 2.2 10^{21} cm^{-2} by 5.6 10^{20} cm^{-2}.

most distant position from the star. However, its kinetic temperature is the highest. This shows that this gas is not heated only by the UV radiation from the star. An additional heating mechanism is required. The morphology and the kinematical structure suggest that it has been heated by the shock produced when the high velocity HI gas impinges into the molecular cloud. Hereafter we will refer to this feature as the "bow-shock" and it is marked with this name in Figs. 2 and 8.

Table 2. Energetics of the outflow

Velocity Range	HI			CO*		
	M	M×v	M×v^2	M	M×v	M×v^2
(kms^{-1})	(M$_\odot$)	(M$_\odot$ kms^{-1})	(M$_\odot$ (kms^{-1})^2)	(M$_\odot$)	(M$_\odot$ kms^{-1})	(M$_\odot$ (kms^{-1})^2)
V $>$ 7.6	0.02	0.10	0.52	0.01	0.06	0.29
V $>$ 7.0	0.06	0.27	1.31	0.04	0.23	1.08
V $>$ 6.4	0.12	0.52	2.25	1.23	4.85	18.9
V $>$ 5.7	0.22	0.83	3.25	6.11	20.5	69.5
V $>$ 5.1	0.37	1.22	4.25	11.9	35.5	108.9
V $>$ 4.4	0.54	1.56	4.90	25.5	61.7	158.7
V $>$ 3.8	0.71	1.78	5.19	81.3	133.6	251.3
V $<$ -4.6	0.05	0.35	2.48			
V $<$ -3.9	0.10	0.65	4.38			
V $<$ -3.3	0.14	0.91	5.90			
V $<$ -2.6	0.18	1.11	6.92			
V $<$ -2.0	0.22	1.31	7.83	0.02	0.10	0.46
V $<$ -1.4	0.26	1.48	8.48	0.10	0.46	1.84
V $<$ -0.7	0.31	1.64	8.99	0.81	2.74	9.18
V $<$ 0.6	0.41	1.87	9.51	21.8	47.5	98.2
V $<$ 1.2	0.48	1.96	9.63	74.1	114.9	185.0
V $<$ 1.2, V $>$ 3.8	1.2	3.7	14.8	155.4	248.5	436.3

* ^{12}CO for V$\leq$ -1 and V$\geq$6 kms^{-1} and ^{13}CO for -1$<$V$<$6 kms^{-1}.

4. The outflow

4.1. Kinematics and geometry of the region

The bipolarity observed in the morphology of ^{12}CO and ^{13}CO emissions suggests that, at least in an earlier evolutionary stage, a bipolar outflow with its axis spatially coincident with the axis of the cavity has been developed in this region. At the present stage, we have no evidence for the existence of atomic and/or molecular high velocity gas along the axis of the cavity. There are some observational problems that could contribute to this fact. Since the outflow is seen almost edge-on, the gas close to the axis would be observed at velocities very close to that of the ambient cloud. This will increase the confusion problems with the foreground gas. However, even in this case one expects to observe the signs of the interaction between the high velocity gas and the molecular cloud. The fact that the bow shock is detected at the tip of one of the HI filaments instead of at the end of the axis of the cavity, support the model in which the high velocity gas is running along the edges of the cavity instead of inside it. Furthermore, two tunnels have been detected in the ^{13}CO integrated intensity emission with the same directions as the HI filaments. As illustrated in Fig. 2, there is a perfect match between the direction and spatial location of the HI filaments and the ^{13}CO tunnels. This strongly suggests that the high velocity gas is mainly flowing along the HI filaments and pushing away the ambient material.

In Fig. 9 we present the velocity-position diagrams of the HI, ^{12}CO and ^{13}CO emission along the strips marked in Fig. 1. Emission at red-shifted and blue-shifted velocities is detected at every position. This is the expected behavior for an edge-on outflow. The highest velocities are observed in the atomic gas located in the vicinity of the star. Within the cavity the high velocity gas is mainly atomic. At the edge of the cavity, intense ^{12}CO emission appears with the same terminal velocity as the HI emission. The bow-shock is located at the interface between the atomic and molecular emission in Strip 2. Deeper into the cloud, the HI emission disappears and the width of the ^{12}CO lines is the same as in the foreground molecular cloud. The width and terminal velocity of both HI and ^{12}CO lines decrease outwards from the star. This kinematical structure is characteristic of a decelerated outflow, in which the velocity of the outflowing gas decreases when it interacts with the ambient cloud.

As commented above, the high velocity HI filaments are only observed towards the eastern lobe. This is also the lobe in which the star is located. Towards the western lobe, we have not detected any HI filaments and there is no evidence of interaction between the ambient gas and high velocity atomic gas. The ^{12}CO lines are narrow and a bow-shock is not found in this lobe. The narrowness of the ^{12}CO lines suggests that the non-detection of the HI filaments in this lobe is not due to observational problems (missing flux in the VLA image) but to a lack of high velocity HI gas in this region.

Summarizing, at the present stage the outflow is mainly formed by atomic gas that is running along the walls of a hollow cone adjacent to the eastern lobe of the cavity. The star is found $\approx 40'' - 50''$ East from the apex of this cone. At the edge of the cavity the atomic gas impinges in the ambient cloud and is decelerated. A layer of shocked molecular gas is formed in the interface between the atomic gas and the ambient cloud.

One expects to find a layered structure in the walls of the cavity with the atomic gas in the inner layers and the molecular gas in the outer ones. Then, the comparison between the

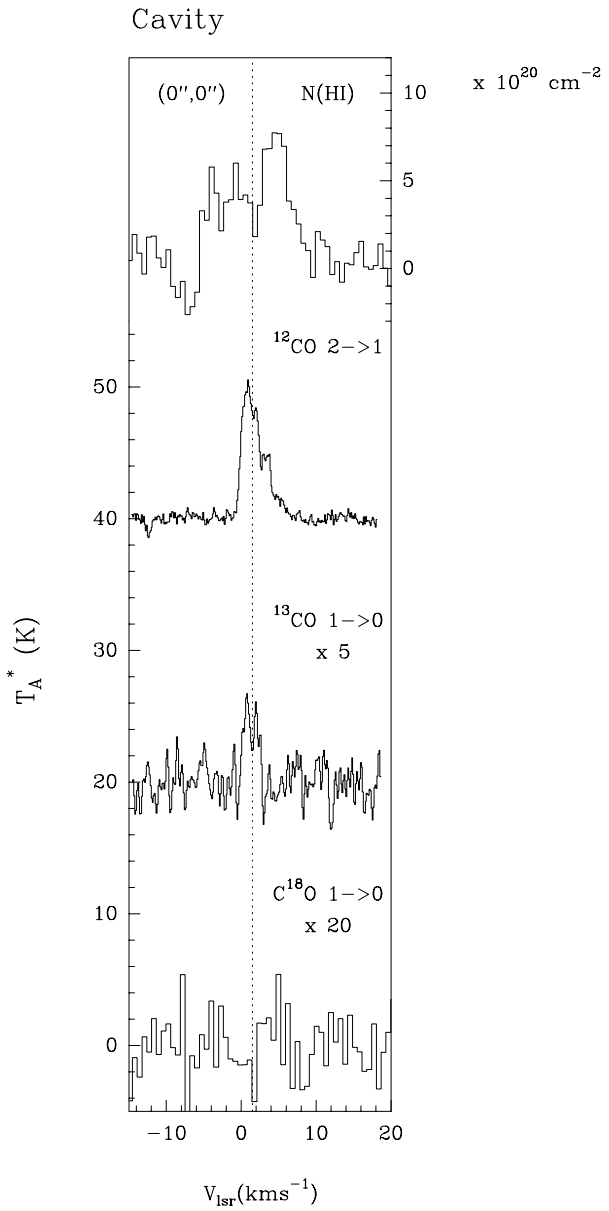

Fig. 6. Spectra of the HI, ^{12}CO J=2→1, ^{13}CO J=1→0 and C^{18}O J=1→0 lines towards the offset (0″,0″). The dashed line indicate the velocity of the ambient cloud (1.5 kms^{-1}).

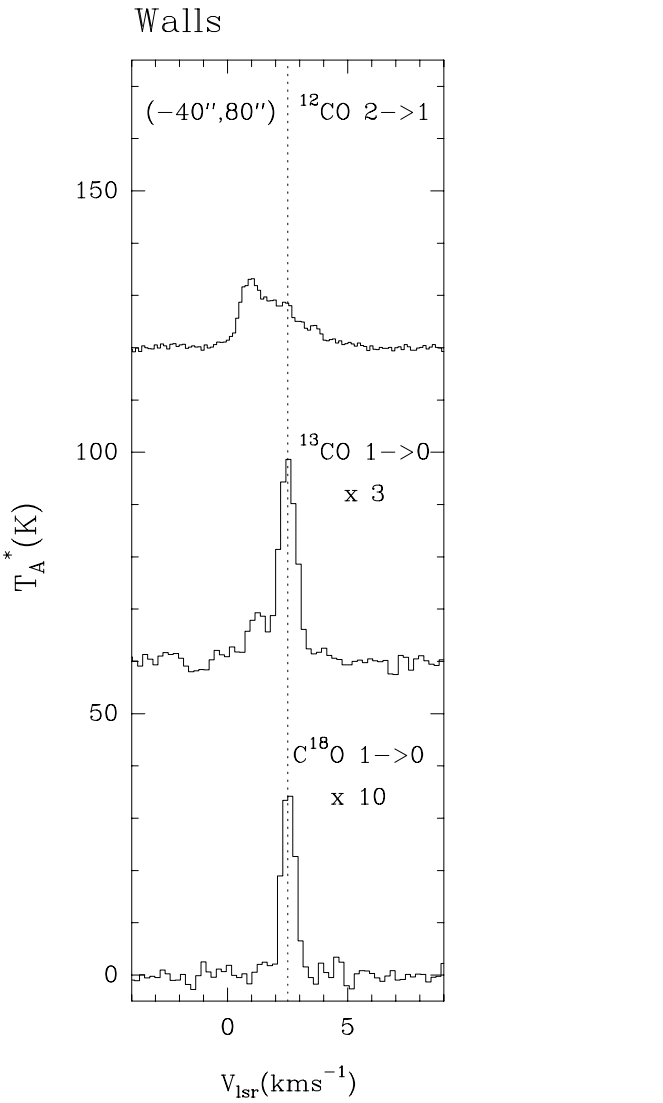

Fig. 7. Spectra of the ^{12}CO J=2→1, ^{13}CO J=1→0 and C^{18}O J=1→0 lines towards the offset (-40″,80″). This position is located in the walls of the cavity.

velocities of the atomic and molecular lines could provide important information about the kinematical structure of the walls. In Fig. 6 we present the HI and molecular spectra towards the star position. The ^{13}CO emission shows a double-peak spectrum with the peaks at $\sim$ 0.7 and 2.0 kms^{-1} and the dip at 1.5 kms^{-1}. This profile is characteristic of an expanding shell with an expansion velocity of $\sim$ 0.6 kms^{-1}. The HI line is wider than the molecular lines. In fact, the HI emission ranges from -5.6 to 8.6 kms^{-1}, with the emission peak at $\sim$ 4 kms^{-1}. This is also the peak of the CII emission (Gerin et al. 1998). However the velocity of the atomic absorption lines is $\sim$ -2 kms^{-1} (Federman et al. 1997). The atomic absorption lines are tracing the atomic layer in front of the star. If we consider the the velocity of the dip in the ^{13}CO spectrum as the reference velocity for the expansion, this layer is expanding at a velocity of $\sim$ 3.5 kms^{-1}. The peaks of the CII and HI emission lines corresponds very likely to the atomic column density peak. According with its velocity, this peak is located in the back wall and is expanding at a velocity of $\sim$ 2.5 kms^{-1}. Comparing the expansion velocities derived from atomic and molecular lines, we conclude that across the walls, the expansion velocity decreases from inside to outside. The aperture of the biconical cavity is $\sim$ 53°. Assuming axial symmetry for the lobes of the cavity and correcting by the inclination angle, we derive that the atomic gas is outflowing with a velocity of $\sim$ 7 kms^{-1} relative to that of the ambient molecular gas at the star position.

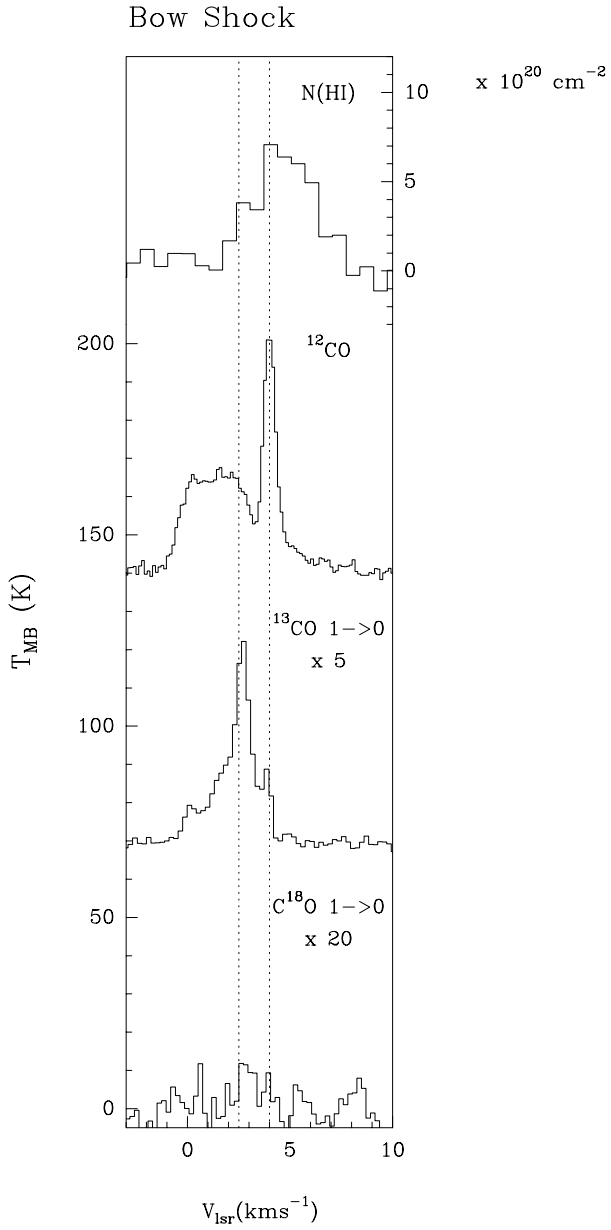

Fig. 8. The same as Fig. 6 for the offset (200″,140″). This offset is the position of the bow-shock. Dashed lines indicate the velocity of the ambient cloud (2.5 kms^{-1}) and that of the bow shock feature (4.0 kms^{-1}). The temperature scale is T_{MB}.

4.2. Energetics

We have estimated the mass, momentum and energy of the high velocity atomic and molecular gas of this outflow. The HI masses have been estimated assuming optically thin emission. To estimate the mass, momentum and energy of the molecular gas we have used our ^{12}CO and ^{13}CO data. Although the ^{12}CO J=2→1 line is self-absorbed at the velocities of the molecular cloud, it is the best tracer for the high velocity gas. We have used the ^{12}CO to estimate the mass of the gas with velocities $\leq$ -1 and $\geq$ 6 kms^{-1}, and ^{13}CO for -1 $\leq$ V $\leq$ 6 kms^{-1}. To estimate the mass of the molecular gas we have assumed optically thin emission, a rotation temperature of 30 K, a standard CO abundance of 8 10^{-5}, and a ^{12}CO/^{13}CO isotopic ratio of 40. The intensity scale is antenna temperature. The main uncertainties in this calculation comes from the assumed rotation temperature and the unknown beam filling factor. The rotation temperature is uncertain by a factor of 2. Relative to the beam-filling factor, although the ^{12}CO is very extended, some high velocity features, like the bow-shock, can have a small angular size. We have used the antenna temperature scale because the contribution to the energetics of the whole region of this thin layer of gas is not very important. In Table 1 we present the mass, momentum and kinetic energy estimates for different velocity intervals.

The momentum in HI is almost 2 orders of magnitude lower than that of the CO outflow. Large uncertainties are involved in these estimates. First of all, an extended component of the HI emission can be missed in our VLA data. Rogers et al. (1995) estimated a total HI mass of $\sim$ 3 M$_\odot$ toward this nebula. Compared with the mass derived from our VLA data, $\sim$ 1.6 M$_\odot$, we could have missed about the 50 % of the total HI flux. Thus, the momentum in HI can be underestimated by a factor of 2. On the other hand, we have not corrected our calculations by the inclination angle relative to the plane of sky. Since the spatial distribution of the ^{12}CO and HI emission are different, we could have a different correction factor for the molecular and the atomic emission. Finally, the HI emission could be optically thick. The HI column densities in the filaments ranges between 3 10^{20} - 2.2 10^{21} cm^{-2}. Assuming a standard value of the spin temperature (T$_s$ = 125 K), the opacity of the HI line would range between 1 and 9. The correction to the HI column densities due to the opacity could be a factor 2 - 9. But even taking into account all these uncertainties, the momentum in the molecular outflow is still an order of magnitude larger than that in HI. The momentum of the HI flux is enough to drive the highest velocity ^{12}CO gas (V $\leq$ -1 and V $\geq$ 6 kms^{-1}) but clearly insufficient to drive the moderate velocity dense gas in the walls of the ^{13}CO cavity. This gas has been very likely accelerated in a previous evolutionary stage when the cavity was excavated by a bipolar ouflow.

From our ^{13}CO data we estimate that the mass in the bright rim that borders the cavity is $\approx$ 800 M$_\odot$. Assuming that the mass was uniformly distributed in the region before the outflow onset, the outflow has swept up $\sim$ 300 M$_\odot$ of molecular gas. We have estimated a dynamical age of $\sim$ 10^5 yrs for the molecular outflow (adopting a size of 0.6 pc and a terminal velocity of 3.5 kms^{-1}). Then, the outflow luminosity is $\sim$ 20 L$\odot$. Cabrit & Bertout (1992) computed the mechanical luminosity of the swept up molecular gas in a sample of outflows driven by sources of very different bolometric luminosity (L$_{bol}\sim$ 1 - 4 10^5 L$_\odot$) and found that both quantities are correlated. The mechanical luminosity estimated in HD 200775 is typical of sources with a bolometric luminosity L$_{bol}\sim$ 10^3 L$_\odot$ (the bolometric luminosity of HD 200775 is L$_{bol}\sim$ 8 10^3 L$_\odot$; van den Ancker et al. 1997). The outflows driven by GL 490, NGC 2071-IRS1 and S140-IRS1 are within this group. However the dynamical ages estimated for these outflows are an order of magnitude lower

than in the case of HD 200775. HD 200775 is very likely one of the oldest intermediate-mass outflows so far studied.

4.3. Around the star

It is natural to think that the star should be located in a clump that is the residual of the core in which it was born. We have not detected any molecular and/or atomic clump at the star position. Although intense HI emission is observed at the star position, the star is not located at a peak in HI column density. In fact it is located at a local minimum, between the two intense HI clumps in the narrow waist of the biconical cavity. Bipolar outflows are thought to have an important role in destroying the parent core. One could think that the outflow has disrupted the initial core and now the star is surrounded by a dense ring perpendicular to the outflow axis. In this scheme, the clumps located in the waist of the cavity are part of this ring. Surprisingly, the star is not found aligned with these clumps. It is displaced $\sim 50''$ East from them. The remnant core has an asymmetric structure with the densest gas located to the west of the star. This structure has also been observed in the interferometric HCO^+ images of the region (Fuente et al. 1996) and in the recent infrared continuum maps obtained by ISO (Cesarsky et al. 1996). Since the same asymmetric spatial distribution is observed in HI, the dust continuum emission and the molecular lines, we conclude that this asymmetry is not the consequence of a chemical effect. It is the consequence of the anisotropic distribution of the material around the star. This asymmetry is also observed in the dust temperature map reported by Rogers et al. (1995). The dust temperature is higher in the eastern lobe than in the western lobe. This is the expected behavior if the extinction is higher towards the west than towards the east because of the anisotropic distribution of the material around the star. In Sect. 5.1, we will propose this anysotropy to explain also the monopolar nature of the HI emission.

5. Discussion

5.1. The model

The existence of a atomic stellar wind as the driving agent of the molecular outflows was very early suggested (Natta et al. 1988), but only the low-mass outflows HH7-11 and L1551 (Giovanaradi et al. 1992), T Tau (Ruiz et al. 1992) and the two high-mass bipolar outflows NGC 7021 (Bally & Stark 1983) and DR21 (Russell et al. 1992) have been detected in HI so far. Other well known outflows, like RNO 43, FU Ori, R Mon, NGC 2264, L1448, have not been detected (Giovanardi et al. 1992). The low-mass stellar outflows HH7-11, L1551, T Tau have been detected using the Arecibo telescope. In these sources the atomic gas reaches velocities up to 150 - 260 kms^{-1} and the momentum supply by the atomic gas can drive the molecular outflow in a momentum conserving interaction. Unfortunately, the low angular resolution of these observations prevent from a study of the spatial distribution of the atomic gas. It was interpreted as a neutral stellar wind that drives the molecular outflow. Toward the high-mass outflows, NGC 2071 and DR 21, the HI 21-cm line has been observed using the VLA. The high velocity atomic gas detected towards NGC 2071 is not able to drive the molecular outflow, and could be due to the photodissociation of the molecular gas by the UV radiation of the recently formed stars. However, towards DR21 Russel et al. (1992) detected a massive (24 $M_\odot$) atomic jet which is capable to drive the massive molecular outflow associated with this source.

The case of HD 200775 seems to be different from that of low-mass stars. The momentum of the atomic outflow is more than two orders of magnitude lower than the momentum of the molecular outflow. Though we cannot discard the possibility of a high velocity atomic wind flowing along the outflow axis, the morphology of the region suggests that this is not the case. Furthermore, we only detect high velocity HI gas in the eastern lobe. Thus the HI gas is not able to drive the molecular outflow at the present stage, and could not have been the driving agent of the outflow which excavated the cavity. We propose that the cavity was formed in an earlier evolutionary stage, and it is, in some sense, a fossil of the bipolar outflow. Most of the molecular gas was accelerated when the cavity was formed and the high velocity atomic gas we observe now drives only the highest velocity molecular gas of the eastern wall (V$>$ 6 kms^{-1} and V$<$ -1 kms^{-1}). The study of the cavity gives important information about the history of the outflow. The four shells observed in ^{12}CO and the symmetry between the two lobes, suggest that at least two episodes of energetic ejections took place along the outflow axis. But it seems that once the central channel was evacuated the high velocity gas started to outflow along the walls of the cavity instead of inside. The tunnels observed in ^{13}CO were very likely formed at this stage. Surprisingly the symmetry of the region is not perfect. The center of symmetry of the multi-shell structure is not located towards the star, but about $40''$– $50''$ (0.08 pc – 0.10 pc) to the west. This is also the position of the waist of the biconical cavity relative to the star. This lack of symmetry is more evident when we study the spatial distribution of gas and dust around the star at a smaller spatial scale. As commented in Sect. 4.3, the circumstellar material is located mainly to the west of the star. Then, the extinction from the star is higher towards the west than towards the east. We propose that this asymmetry is the responsible of the cometary shape of the HI outflow. First, because of the lower extinction towards the eastern lobe, the heating and photodissociation of the gas by the stellar UV radiation is producing mainly in this lobe. Secondly, the HI outflow could be driven by an isotropic stellar wind. In this case, the stellar wind would impinge to the west in a dense wall and turn back to the east producing a cometary outflow. This model is illustrated in Fig. 10.

5.2. The origin of a cometary nebula

In Sect. 5.1 we propose that the cometary shape of the HI emission is the consequence of an asymmetric distribution of matter around the star. But it is difficult to justify this asymmetric distribution if the disruption of the core has been produced by the bipolar outflow. At some point the bipolar symmetry disappeared. Two scenarios are proposed to account for this change: i)

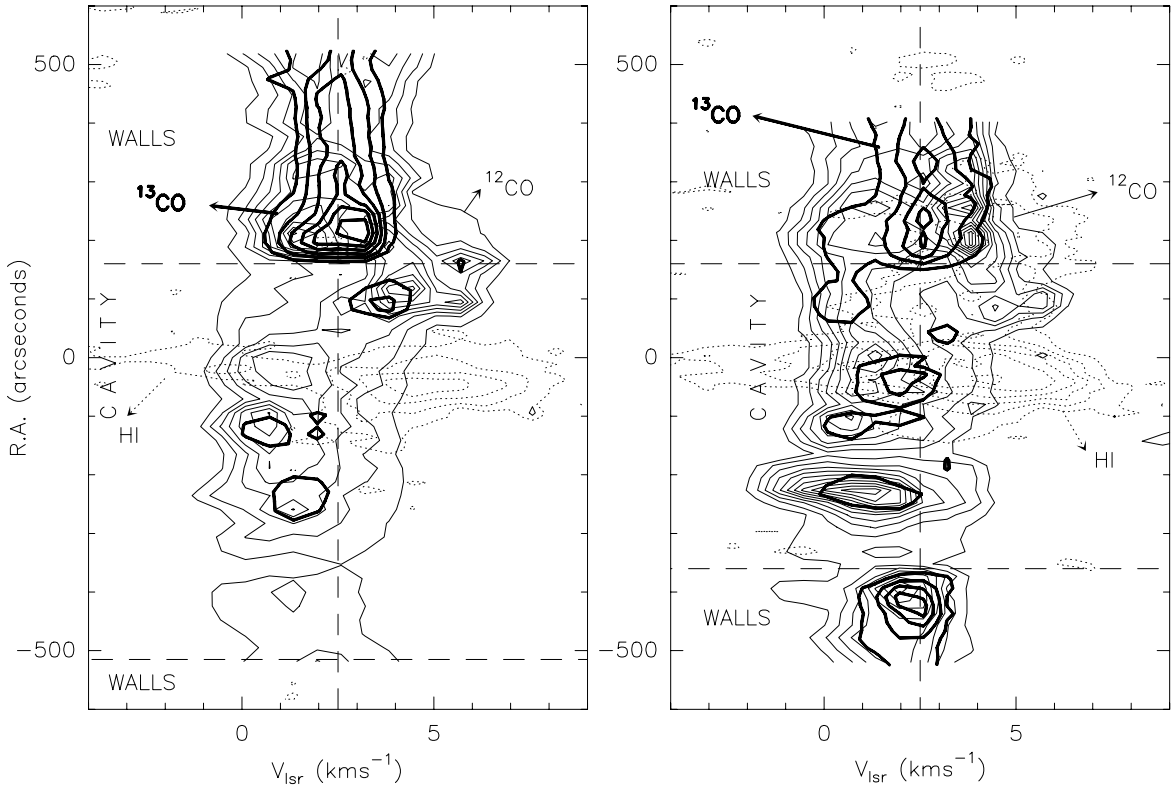

Fig. 9. Velocity-position diagram of the emission of the ^{12}CO J=2→1 and ^{13}CO J=1→0 lines and the HI column density for strip 1 and 2 (see Fig. 1). Contour levels are: 1.6 to 20.8 by 1.6 K for the ^{12}CO J=2→1 line; 1 to 10 by 1 K for the ^{13}CO J=1→0 line and 3.4 10^{20} to 2.2 10^{21} by 3.4 10^{20} cm^{-2}. To have the same velocity resolution for the three emissions, we have degraded the resolution of the ^{12}CO and ^{13}CO data to 0.644 kms^{-1}.

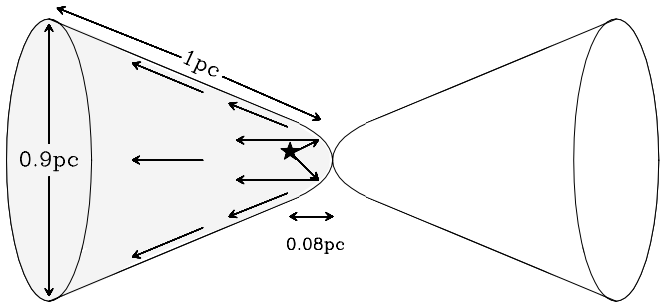

Fig. 10. Illustrative scheme of the model proposed in Sect. 5.1. The star is heating and photodissociating mainly the eastern lobe. For clearness, the scale is not real.

The existence of a binary could have introduced asymmetries in the disruption of the parent core. A close companion has been detected for this star by Pirzkal et al. (1997). ii) The star has moved away from its initial position. Once the bipolar outflow excavated the cavity, the star could have wandered to the east. Then the dispersal of material would be more efficient to the east than to the west producing an anisotropic distribution of the matter surrounding the star. The advantage of the latter explanation is that it can account for the "strange" position of the star relative to the biconical cavity . Both, the multi-shell structure observed in ^{12}CO and the biconical cavity seem to be centered in a position located 40″– 50″ (0.08 pc – 0.10 pc) to the west of the star. It seems as if the exciting star of the initial bipolar outflow were located at this position instead of at the position of HD 200775. One could think that HD 200775 is not responsible for the cavity. A possible low-mass companion located at the waist of the cavity could have produced it. This explanation is very unlikely. There is no evidence for the existence of a star around this position (see Sellgren et al. 1983). Furthermore, the amount of material swept up by the outflow suggests that the cavity has been formed by an intermediate-mass star (see Sect. 4.2). It is more plausible to think that the biconical cavity was excavated by HD 200775 and the star has changed its position. The proper motions of HD 200775 are ($\mu_\alpha cos(\delta)$, μ_δ) = (+6.74 $\pm$ 0.64 mas yr^{-1}, -1.48 $\pm$ 0.54 mas yr^{-1}) (from Hipparcos Catalogue). The direction of these motions is in agreement with the observed displacement. In $\sim$ 3000 yrs the star could have moved from the center of symmetry of the bipolar outflow to its position nowadays. This time is negligible compared to the age of the outflow ($\sim$ 10^5 yrs). We are aware that the proper motions measure the absolute motions of the star and do not give any information about the relative motion of the star with respect to the surrounding cloud. Both, the star and the parent molecular cloud could be moving at the same velocity. To have an estimate of this motion, we have compared the velocity of the star with that of the molecular gas in its surroundings. Finkezellet & Mundt (1984)

obtained that the difference in velocity between the star and the molecular cloud is 3 kms^{-1}. At the distance of HD 200775, a velocity of 3 kms^{-1} would correspond to $\sim$ 1 mas yr^{-1}. This velocity is of the same order as the measured proper motions. Of course, there is a great uncertainty in the velocity of the star and consequently in this number. But the existence of a shift in radial velocity proves, at least, that the model is plausible. Cometary nebulae and cometary HII regions are very common in the interstellar medium. If intermediate-mass and massive star moves away from their initial position in the last stages of the mass-loss phase, the cometary shape of these regions has an easy and simple explanation. A similar observational work in other cometary nebulae is required to check this hypothesis.

6. Summary and conclusions

In this paper, we present a kinematical study of the molecular and atomic gas of the bipolar outflow associated to HD 200775. Our results can be summarized as follows:

- The star is located in a biconical cavity of $\sim$ 1.5 pc $\times$ 0.8 pc. The shape of this cavity, as observed in ^{12}CO and ^{13}CO emissions, suggests that it has been excavated by a bipolar outflow. Within the cavity the gas is mainly atomic.
- There is no evidence for high velocity gas within the cavity. Two HI filaments are detected adjacent to the walls of the cavity in the eastern lobe. A bow shock is found at the tip of one of these filaments. These filaments are very likely high velocity atomic gas that is outflowing at the edges of the cavity. We have not detected any HI filaments in the western lobe.
- The spatial distribution of the material around the exciting star is not symmetric. The extinction from the star to the western lobe seems to be higher than towards the eastern one. This asymmetric distribution of matter around the star is very likely the responsible of the higher dust temperature found in the eastern lobe and of the asymmetric spatial distribution of the HI emission.
- We propose that the outflow associated with HD 200775 is in the latest stage of its evolution. Although it was clearly bipolar in previous evolutionary stages, now it is very likely driven by an isotropic wind. To the west, this wind collides with a dense wall producing a cometary outflow.
- The asymmetric distribution of matter around the star is easily explained if the star has moved away from its initial position during the outflow evolution.

Acknowledgements. We are grateful to the technical staff of Pico de Veleta for their support during the observations. This work has been partially supported by the Spanish DGES under grant number PB96-0104.

References

Bachiller R., 1996 ARA & A 34, 111
Bally J., Stark A.A., 1983 ApJ 266, L61
Blouin, D., Mccutcheon, W.H., Dewdney, P.E., Roger, R.S., Purton, C.R., Kester, D., Bontekde, TJ.R., 1997 MNRAS 287,455
Cabrit S., Bertout C., 1992, A & A 261, 274
Catala, 1989, in Low Mass Star Formation and Pre-Main Sequence Evolution, ed. B. Reipurth (Garching: ESO), 471
Cesarsky D., Lequeux J., Abergel A., Perault M., Palaxxi E., Madden S., Tran D., 1996 A & A 315, L305
Federman S.R., Knauth D.C., Lambert D.L., Andersson B.G., 1997 ApJ 489, 758
Finkenzeller U., & Mundt R., 1984 A & AS 57, 285
Fuente A., Martín-Pintado J., Cernicharo J., Brouillet N., Duvert G., 1992 A & A 260, 341
Fuente A., Martín-Pintado J., Cernicharo J., Bachiller R., 1993, A & A 276, 473
Fuente A., Martín-Pintado J., Neri R., Rogers C., Moriarty-Schieven G., 1996 A & A 310, 286
Fuente A., Martín-Pintado J., Bachiller R., Neri R., Palla F., 1998 A & A 334, 253
Gerin M., Phillips T.G., Keene J., Betz A.L., Boreiko R.T., 1998 ApJ 500, 329
Giovanardi C., Lizano S., Natta A., Evans N.J. II, 1992 ApJ 397, 214
Grillo F., Sciortino S., Micela G., Vaiana G.S., Harnden F.R., 1992 ApJS 81, 795
Lizano S., Heiles C., Rodríguez L.F., Koo B-C, Shu F.H., Hasegawa T., Hayashi S., Mirabel I.F., 1988 ApJ 328, 763.
Natta A., Giovanardi C., Palla F., Evans N.J.II, 1988 ApJ 327, 817
Pirzkal N., Spillar E.J., Dyck H.M., 1997 ApJ 481, 392
Proust D., Ochsenbein F., Pettersen B.R., 1981 A & AS 44, 179
Rogers C., Heyer M.H., Dewdney P.E., 1995 ApJ 442, 694
Ruiz A., Alonso J.L., Mirabel I.F., 1992, ApJ 394, L57
Russell A.P.G., Bally J., Padman R., Hills R.E., 1992 ApJ 387, 219
Sanders W.T., Cassinelli J.P., & Anderson C.M., 1982 BAAS 14,6
Skinner S.L., Brown A., Stewart R.T., 1993 ApJS 87, 217
Strom K.M. et al., 1990 ApJ 362, 168
Sellgren K., 1983 AJ 88, 985
van den Ancker M.E., Thé P.S., Tjin A Djie H.R.E., Catala C., de Winter D., Blondel P.F.C., Waters L.B.F.M., 1997 A & A 324, L33
Watt G.D., Burton W.B., Choe S.-U., Liszt H.S., 1986 å 163, 194
Whitcomb S.E., Gately I., Hildebrand R.H., Keene J., Sellgren K., Werner M.W., 1981, ApJ 246, 416